DOI: 10.7641/CTA.2015.50353

多无人机航迹融合算法及性能评估

陆科林[1†], 周　锐[1], 张翔伦[2]

(1. 北京航空航天大学 自动化科学与电气工程学院, 北京 100191; 2. 西安自动飞行控制研究所, 陕西 西安 710065)

摘要: 航迹融合是多无人机系统进行协同侦察, 巡逻和目标跟踪领域中的一个重要问题. 本文根据不同信息反馈配置给出了局部航迹之间的协方差的精确计算, 并据此提出一种精确、具有可扩展性并且适用于任意通信频率的航迹融合算法. 此外, 本文通过求解对应的离散代数Riccati方程求取融合估计的稳态误差协方差, 并以此进行融合性能分析. 最后, 本文利用Monte Carlo仿真比较理论和实际结果, 实验结果验证了该融合算法的有效性.

关键词: 航迹融合; 无人机; 卡尔曼滤波器; 目标跟踪; 估计

中图分类号: V279　　　**文献标识码**: A

Exact algorithms for track-to-track fusion by multiple UAVs and performance evaluation

LU Ke-lin[1†], ZHOU Rui[1], ZHANG Xiang-lun[2]

(1. School of Automation Science and Electrical Engineering, Beihang University, Beijing 100191, China;
2. AVIC Automatic Flight Control Research Institute, Xi'an Shaanxi 710065, China)

Abstract: Track-to-track fusion is an important topic for cooperative surveillance, reconnaissance and target tracking by multiple unmanned aerial vehicles (UAVs). In this paper, the accurate cross-covariances between the local estimates are obtained from various information feedback configurations, which gives rise to the scalable and consistent algorithms for track-to-track fusion (T2TF) at an arbitrary communication rate. Furthermore, the steady-state error covariance of the fused estimate is obtained by solving the corresponding discrete algebraic Riccati equation for performance analysis. In addition, the theoretical results are compared with those from the extensive Monte Carlo simulation, which validates the effectiveness of the proposed fusion algorithms.

Key words: track-to-track fusion; unmanned aerial vehicles; Kalman filters; target tracking; estimation

1 Introduction

For the problem of cooperative tracking of a moving target by multiple unmanned aerial vehicles (UAVs)[1], where each UAV is able to track the target with active or passive sensors equipped on it, the optimal result of data fusion is from the centralized measurement fusion (CMF)[2], where all the measurements are sent from the UAVs to the fusion center (FC). The FC could be collocated with a leader UAV, otherwise it is a remote station. For CMF, the FC uses a centralized Kalman filter[3] to estimate the target track, however it is not practical due to its high communication requirements. An alternative manner for sensor fusion is to adopt the track-to-track fusion (T2TF)[4], where the FC fuses the local estimated tracks instead of the raw measurements. Compared with CMF, the major advantage of T2TF is that it could effectively reduce the frequency of communication and perform at a lower rate[5]. The problem of track-to-track correlation due to the common process noise has been observed in [6], and the T2TF accounting for the correlated tracks has been developed in [7] by making use of a static linear estimation model[8]. In [9] the author has proved that the result from [7] is approximate and only optimal in the maximum likelihood (ML) sense. The information matrix filter (IMF)[10] is another type of the T2TF algorithm, unlike the one-scan algorithm developed in [7], the IMF is multi-scanned, which means that it also fuses tracks from the previous fusion steps. Besides, the fuser does not require the cross-covariances between the local tracks, which is well known to be difficult to calculate[11]. However, it is to be noted that the IMF is optimal only at the full communication rate[12]. The

Received 30 April 2015; accepted 19 July 2015.

†Corresponding author. E-mail: klu@buaa.edu.cn; Tel.: +86 18611242591.

Supported by National Natural Science Foundation of China (61273349, 61175109, 61203223), and the Aviation Science Foundation of China (2013ZA18001, 2014ZA18004).

major challenge in T2TF problems lies in the treatment of the correlations between the local tracks to be fused, otherwise the derived fusion algorithms[13] might be not consistent.

Despite all the above research efforts, there has been very limited studies on the simultaneous fusion of multiple tracks, thus it remains an open topic of research to provide a solution for the cooperative tracking problem by multiple UAVs. Although it has been mentioned in [14] that there is no theoretical limit on the number of local tracks to fuse, from which the derived result still only applies to the two-track case. For these reasons, developing scalable and consistent T2TF algorithms is the focus of this paper. Our major contributions include exact calculation of cross-covariances between multiple local tracks and the corresponding performance evaluation via the theoretical analysis and extensive Monte Carlo simulations.

2 Problem formulation

Consider a scenario with N UAVs tracking a moving target, where each UAV estimates the target track with its local estimator. Assume that each UAV is allowed to send its latest estimation to the FC with an identical interval T. The UAV may or may not receive the feedback from the FC according to different information feedback configurations. In this paper, the out-of-sequence problem[15] is omitted for the sake of brevity, that is, the communication links between the UAVs and FC is assumed without delay and no data loss. At the FC, let $\hat{x}_{\rm c}$, $P_{\rm c}$ represent the fused track, and $P_{s_is_j}$ represent the cross-covariance between the local tracks, then the fusion of the local tracks at step k is formulated as follows:

$$\begin{aligned}&[\hat{x}_{\rm c}(k|k), P_{\rm c}(k|k)] = \\ &f(\{\hat{x}_{s_i}(k|k)\}, \{P_{s_i}(k|k)\}, \{P_{s_is_j}(k|k)\}),\end{aligned} \tag{1}$$

where $s_i, s_j = 1, \cdots, N$ and $s_i \neq s_j$. Note that once an UAV s_i receives a feedback from the FC, its local track is updated to $\hat{x}^*_{s_i}(k|k)$ and $P^*_{s_i}(k|k)$, and the cross-covariances stored in the FC are also updated to $P^*_{s_is_j}(k|k)$ accordingly. Various patterns of information feedback configurations will be considered in the next section, including no feedback, partial feedback and full feedback.

3 T2TF algorithms for different information feedback configurations

Assume that the local tracks $\{\hat{x}_{s_i}(k|k)\}$, $\{P_{s_i}(k|k)\}$ and the cross-covariances $\{P_{s_is_j}(k|k)\}$ are available at FC, the optimal fusion in the maximum likelihood (ML)[2] sense can be performed according to the following formulas:

$$\hat{x}_{\rm c} = (I_N^{\rm T} P_N^{-1} I_N)^{-1} I_N^{\rm T} P_N^{-1} \hat{X}_N, \tag{2}$$

$$P_{\rm c} = (I_N^{\rm T} P_N^{-1} I_N)^{-1}, \tag{3}$$

where I is an $n \times n$ identity matrix, $I_N = [I \; I \; \cdots \; I]$ is an $Nn \times n$ matrix, $\hat{X}_N = [\hat{x}_1 \; \hat{x}_2 \; \cdots \; \hat{x}_N]^{\rm T}$ and P_N is an $Nn \times Nn$ matrix with the following blocks:

$$P_N = \begin{bmatrix} P_1 & P_{12} & \cdots & P_{1N} \\ P_{21} & P_2 & \cdots & P_{2N} \\ \vdots & \vdots & & \vdots \\ P_{N1} & P_{N2} & \cdots & P_N \end{bmatrix}. \tag{4}$$

Assume that the previous fusion is performed at time step l, then we have

$$\tilde{x}^*_{s_i}(l|l) = \hat{x}^*_{s_i}(l|l) - x(l), \tag{5}$$

where $x(l)$ represents the true state of the target. It can be further derived that

$$\begin{aligned}\tilde{x}_{s_i}(l+1|l+1) = &(I - K_{s_i}(l+1)H)A\tilde{x}_{s_i}(l|l) - \\ &(I - K_{s_i}(l+1)H)w(l) + \\ &K_{s_i}(l+1)v_{s_i}(l+1),\end{aligned} \tag{6}$$

where K_{s_i} is the Kalman filter gain for the s_ith local estimator, H is the observation matrix and A is the state transition matrix. The following formula will be used to update the filter residual, which is obtained by using (6) recursively for all the local tracks from the time step l to k:

$$\begin{aligned}\tilde{x}_{s_i}(k|k) = &W^{\rm e}_{s_i}(d,l)\tilde{x}^*_{s_i}(l|l) + \\ &\sum_{i=1}^{d} W^{\rm v}_{s_i}(i,d,l)w(l+i-1) + \\ &\sum_{i=1}^{d} W^{\rm w}_{s_i}(i,d,l)v_{s_i}(l+i),\end{aligned} \tag{7}$$

where $d = k - l$ and the weights are derived as

$$W^{\rm e}_{s_i}(i,d,l) = \sum_{i=1}^{d}(I - K_{s_i}(l+i)H)A,$$

$$W^{\rm v}_{s_i}(i,d,l) = \begin{cases} -(I - K_{s_i}(l+i)H), \; d-i=0, \\ -\prod\limits_{j=1}^{d-i}((I - K_{s_i}(l+d-j+1)H)A)\times \\ (I - K_{s_i}(l+i)H), \quad d-i \geqslant 1, \end{cases}$$

$$W^{\rm w}_{s_i}(i,d,l) = \begin{cases} K_{s_i}(l+i), \; d-i=0, \\ \prod\limits_{j=1}^{d-i}((I - K_{s_i}(l+d-j+1)H)A)K_{s_i}(l+i), \\ \qquad d-i \geqslant 1. \end{cases}$$

Then the cross-covariance between any two local tracks can be calculated with (7) as

$$P_{s_is_j}(k|k) = W^{\mathrm{e}}_{s_i}(d,l)P^*_{s_is_j}(l|l)(W^{\mathrm{e}}_{s_j}(d,l))^{\mathrm{T}} + \sum_{i=1}^{d} W^{\mathrm{v}}_{s_i}(i,d,l)Q(W^{\mathrm{v}}_{s_j}(i,d,l))^{\mathrm{T}}, \quad (8)$$

where Q is the covariance of the process noise.

For different information feedback configurations, the exact calculation of cross-covariances is given in the following.

For the configuration of no feedback, we have

$$\hat{x}^*_{s_i}(k|k) = \hat{x}_{s_i}(k|k), \quad (9)$$

$$P^*_{s_i}(k|k) = P_{s_i}(k|k), \quad (10)$$

$$P^*_{s_is_j}(k|k) = P_{s_is_j}(k|k), \quad (11)$$

where $P_{s_is_j}$ is given as (8).

For the configuration of full feedback, we have

$$\hat{x}^*_{s_i}(k|k) = \hat{x}_{\mathrm{c}}(k|k), \quad (12)$$

$$P^*_{s_i}(k|k) = P_{\mathrm{c}}(k|k), \quad (13)$$

$$P^*_{s_is_j}(k|k) = P_{\mathrm{c}}(k|k), \quad (14)$$

where $\hat{x}_{\mathrm{c}}$ and P_{c} are given as (2) and (3).

For the configuration of partial feedback, it requires to account for four different cases, which are shown as follows:

Case 1 Both UAV s_i and UAV s_j receive the feedback from FC.

Case 2 Neither UAV s_i nor UAV s_j receives the feedback from FC.

Case 3 UAV s_i receives the feedback but UAV s_j receives no feedback from FC.

Case 4 UAV s_i receives no feedback but UAV s_j receives the feedback from FC.

It is straightforward that (11) and (14) could be used to calculate the updated cross-covariance $P^*_{s_is_j}$ for Case 1 and Case 2 respectively. The formulas for the rest two cases are derived as follows:

Theorem 1 If UAV s_i receives the feedback but UAV s_j receives no feedback from FC, then

$$P^*_{s_is_j}(k|k) = (I_N^{\mathrm{T}}P_N^{-1}I_N)^{-1}(I_N^{\mathrm{T}}P_N^{-1}) \begin{pmatrix} P_{1s_j} \\ P_{2s_j} \\ \vdots \\ P_{Ns_j} \end{pmatrix}. \quad (15)$$

Proof The fused error is defined as

$$\tilde{x}_{\mathrm{c}} = \hat{x}_{\mathrm{c}} - x. \quad (16)$$

By Substituting (2) into (16) it gives that

$$\begin{aligned}\tilde{x}_{\mathrm{c}} = {} & (I_N^{\mathrm{T}}P_N^{-1}I_N)^{-1}I_N^{\mathrm{T}}P_N^{-1}\hat{X}_N - x = \\ & (I_N^{\mathrm{T}}P_N^{-1}I_N)^{-1}I_N^{\mathrm{T}}P_N^{-1}\hat{X}_N - \\ & (I_N^{\mathrm{T}}P_N^{-1}I_N)^{-1}(I_N^{\mathrm{T}}P_N^{-1}I_N)x = \\ & (I_N^{\mathrm{T}}P_N^{-1}I_N)^{-1}(I_N^{\mathrm{T}}P_N^{-1}\hat{X}_N - I_N^{\mathrm{T}}P_N^{-1}I_Nx) = \\ & (I_N^{\mathrm{T}}P_N^{-1}I_N)^{-1}(I_N^{\mathrm{T}}P_N^{-1})(\hat{X}_N - I_Nx) = \\ & (I_N^{\mathrm{T}}P_N^{-1}I_N)^{-1}(I_N^{\mathrm{T}}P_N{-}1)\tilde{X}_N, \end{aligned} \quad (17)$$

where

$$\tilde{X}_N = \begin{pmatrix} \tilde{x}_1 \\ \tilde{x}_2 \\ \vdots \\ \tilde{x}_N \end{pmatrix}. \quad (18)$$

Let

$$P^*_{s_is_j}(k|k) = \mathrm{Cov}(\tilde{x}^*_{s_i},\ \tilde{x}^*_{s_j}). \quad (19)$$

Recall that for Case 3 we have

$$\hat{x}^*_{s_i}(k|k) = \hat{x}_{\mathrm{c}}(k|k), \quad (20)$$

and

$$\hat{x}^*_{s_j}(k|k) = \hat{x}_{s_j}(k|k). \quad (21)$$

By substituing (20) and (21) into (19) it gives that

$$\begin{aligned} & P^*_{s_is_j}(k|k) = \\ & \mathrm{E}((I_N^{\mathrm{T}}P_N^{-1}I_N)^{-1}(I_N^{\mathrm{T}}P_N^{-1})\tilde{X}_N\tilde{x}^{\mathrm{T}}_{s_j}) = \\ & (I_N^{\mathrm{T}}P_N^{-1}I_N)^{-1}(I_N^{\mathrm{T}}P_N^{-1})\mathrm{E}(\tilde{X}_N\tilde{x}^{\mathrm{T}}_{s_j}) = \\ & (I_N^{\mathrm{T}}P_N^{-1}I_N)^{-1}(I_N^{\mathrm{T}}P_N^{-1})\mathrm{E}\left(\begin{pmatrix} \tilde{x}_1 \\ \tilde{x}_2 \\ \vdots \\ \tilde{x}_N \end{pmatrix}\tilde{x}^{\mathrm{T}}_{s_j}\right) = \\ & (I_N^{\mathrm{T}}P_N^{-1}I_N)^{-1}(I_N^{\mathrm{T}}P_N^{-1})\begin{pmatrix} \mathrm{E}(\tilde{x}_1\tilde{x}^{\mathrm{T}}_{s_j}) \\ \mathrm{E}(\tilde{x}_2\tilde{x}^{\mathrm{T}}_{s_j}) \\ \vdots \\ \mathrm{E}(\tilde{x}_N\tilde{x}^{\mathrm{T}}_{s_j}) \end{pmatrix} = \\ & (I_N^{\mathrm{T}}P_N^{-1}I_N)^{-1}(I_N^{\mathrm{T}}P_N^{-1})\begin{pmatrix} P_{1s_j} \\ P_{2s_j} \\ \vdots \\ P_{Ns_j} \end{pmatrix}. \end{aligned} \quad (22)$$

The proof is completed.

Theorem 2 If UAV s_i receives no feedback but UAV s_j receives the feedback from FC, then

$$P^*_{s_is_j}(k|k) = \begin{pmatrix} P_{1s_i} \\ P_{2s_i} \\ \vdots \\ P_{Ns_i} \end{pmatrix}^{\mathrm{T}} (I_N^{\mathrm{T}}P_N^{-1})^{\mathrm{T}} \times [(I_N^{\mathrm{T}}P_N^{-1}I_N)^{-1}]^{\mathrm{T}}. \quad (23)$$

Proof

$$\begin{aligned} & P^*_{s_is_j}(k|k) = \mathrm{Cov}(\tilde{x}^*_{s_i}, \tilde{x}^*_{s_j}) = \mathrm{E}(\tilde{x}^*_{s_i}(\tilde{x}^*_{s_j})^{\mathrm{T}}) = \\ & \mathrm{E}((\tilde{x}^*_{s_j}(\tilde{x}^*_{s_i})^{\mathrm{T}})^{\mathrm{T}}) = (\mathrm{E}(\tilde{x}^*_{s_j}(\tilde{x}^*_{s_i})^{\mathrm{T}}))^{\mathrm{T}} = \\ & (\mathrm{Cov}(\tilde{x}^*_{s_j}, \tilde{x}^*_{s_i}))^{\mathrm{T}} = (P^*_{s_js_i}(k|k))^{\mathrm{T}}. \end{aligned} \quad (24)$$

By applying Theorem 1 it gives that

$$P^*_{s_is_j}(k|k) = (P^*_{s_js_i}(k|k))^{\mathrm{T}} = \begin{pmatrix} P_{1s_i} \\ P_{2s_i} \\ \vdots \\ P_{Ns_i} \end{pmatrix}^{\mathrm{T}} (I_N^{\mathrm{T}} P_N^{-1})^{\mathrm{T}} \times [(I_N^{\mathrm{T}} P_N^{-1} I_N)^{-1}]^{\mathrm{T}}. \quad (25)$$

The proof is completed.

4 Steady-state performance prediction

In this section, the theoretical performance of the developed fusion algorithms are evaluated in terms of the steady-state mean square error (MSE) covariance, namely,

$$\Omega = \lim_{k\to\infty} \mathrm{E}(\tilde{x}_{\mathrm{c}}(k|k)\tilde{x}_{\mathrm{c}}^{\mathrm{T}}(k|k)) = \mathrm{E}(\tilde{x}_{\mathrm{c}}\tilde{x}_{\mathrm{c}}^{\mathrm{T}}), \quad (26)$$

where $\tilde{x}_{\mathrm{c}}$ is given in (16). Let the dynamic system follow the model as

$$x(k) = Ax(k-1) + w(k-1), \quad (27)$$

where $x = (x, \dot{x})^{\mathrm{T}}$. And the observation system is modeled as

$$z_{s_i}(k) = Hx(k) + v_{s_i}(k), \quad (28)$$

where $v_{s_i}(k) \sim N(0, R_{s_i})$. Define $K_{s_i}(k)$ as the local Kalman gain, $\hat{x}_{s_i}(k|k-1)$ as the local prior state estimate and $P_{s_i}(k|k-1)$ as the prior filter covariance at time step k. In steady state, let

$$K_{s_i} = \lim_{k\to\infty} P_{s_i}(k|k-1), \quad (29)$$

$$\bar{P}_{s_i} = \lim_{k\to\infty} P_{s_i}(k|k-1), \quad (30)$$

$$P_{s_i} = \lim_{k\to\infty} P_{s_i}(k|k), \quad (31)$$

$$P_{s_is_j} = \lim_{k\to\infty} P_{s_is_j}(k|k), \quad (32)$$

$$P_{\mathrm{c}} = \lim_{k\to\infty} P_{\mathrm{c}}(k|k). \quad (33)$$

4.1 Two-track case

The performance of the fusion algorithms is first evaluated for the two-track case. After that, the results will be expanded for arbitrary number of local tracks in the next subsection.

Suppose that there are two local tracks, then the fusion rule, namely (2) and (3) could be rewritten as[7]

$$\hat{x}_{\mathrm{c}} = \hat{x}_1 + K_{12}(\hat{x}_2 - \hat{x}_1), \quad (34)$$

$$P_{\mathrm{c}} = P_1 - K_{12}(P_1 - P_{21}), \quad (35)$$

where

$$K_{12} = (P_1 - P_{12})(P_1 + P_2 - P_{12} - P_{21})^{-1}. \quad (36)$$

By substituting (34) into (16), the fused error is derived as

$$\tilde{x}_{\mathrm{c}} = (I - K_{12})\tilde{x}_1 + K_{12}\tilde{x}_2. \quad (37)$$

By substituting (37) into (26) it gives that

$$\begin{aligned}\Omega = {} & (I-K_{12})P_1(I-K_{12})^{\mathrm{T}} + \\ & (I-K_{12})P_{12}(K_{12})^{\mathrm{T}} + \\ & K_{12}P_{21}(I-K_{12})^{\mathrm{T}} + K_{12}P_2(K_{12})^{\mathrm{T}}. \quad (38)\end{aligned}$$

In the following, Ω is derived for the information feedback configuration of no feedback and full feedback. The results for partial feedback is omitted for the sake of brevity, since the number of UAVs which are supposed to receive the feedback may be varying for the partial feedback configuration, besides it has been proved that its performance is between the other two configurations[14].

4.1.1 No feedback

Suppose that there is no feedback from the FC, then the following steady-state Kalman filter equation is obtained for all the local estimators,

$$\bar{P}_{s_i} = AP_{s_i}A^{\mathrm{T}} + Q, \quad (39)$$

$$K_{s_i} = \bar{P}_{s_i}H^{\mathrm{T}}(H\bar{P}_{s_i}H^{\mathrm{T}} + R_{s_i})^{-1}, \quad (40)$$

$$P_{s_i} = (I - K_{s_i}H)\bar{P}_{s_i}. \quad (41)$$

By substituting (39) and (40) into (41) it gives that

$$\begin{aligned}& (I - (AP_{s_i}A^{\mathrm{T}} + Q)H^{\mathrm{T}}(H(AP_{s_i}A^{\mathrm{T}} + Q) \times \\ & H^{\mathrm{T}} + R_{s_i})^{-1}H) \times \\ & (AP_{s_i}A^{\mathrm{T}} + Q) - P_{s_i} = 0. \quad (42)\end{aligned}$$

Then P_{s_i} can be obtained by solving the above algebraic Riccati equation. After that $\bar{P}_{s_i}$ and K_{s_i} can be calculated with (39) and (40) respectively. Besides, for the cross-covariance we have

$$P_{12} = W_1^{\mathrm{e}}P_{12}(W_2^{\mathrm{e}})^{\mathrm{T}} + \sum_{i=1}^{d} W_1^{\mathrm{v}}(i)Q(W_2^{\mathrm{v}}(i))^{\mathrm{T}}. \quad (43)$$

Hence P_{12} can be obtained in a similar manner by solving (43) given K_{s_i}. And finally we can obtain K_{12} and Ω with (36) and (38) respectively.

4.1.2 Full feedback

Suppose that the fusion is performed at the time step $k-d$, then the following equations are obtained at the time step $k-d+1$,

$$\begin{aligned}& P_{s_i}(k-d+1|k-d) = \\ & AP^*_{s_i}(k-d|k-d)A^{\mathrm{T}} + Q = \\ & AP_{s_i}(k-d|k-d)A^{\mathrm{T}} + Q, \quad (44)\end{aligned}$$

$$\begin{aligned}& P_{s_i}(k-d+1|k-d|1) = \\ & (I - K_{s_i}(k-d+1)H)P_{s_i}(k-d+1|k-d), \quad (45)\end{aligned}$$

where

$$\begin{aligned}& K_{s_i}(k-d+1) = \\ & P_{s_i}(k-d+1|k-d)H^{\mathrm{T}} \times \\ & (HP_{s_i}(k-d+1|k-d) \times H^{\mathrm{T}} + R_{s_i})^{-1}. \quad (46)\end{aligned}$$

Since the next fusion happens at time step k, here we can update $P_{s_i}(\cdot|\cdot)$ recursively from time step $k-d+2$ to k. In this manner, a function is obtained to determine the relation between $\bar{P}_{s_i}$ and $P_{\rm c}$ as

$$\bar{P}_{s_i} = f(P_{\rm c}). \tag{47}$$

For example, if $d=2$, then in steady-state

$$\bar{P}_{s_i} = A(I-(AP_{\rm c}A^{\rm T}+Q)H^{\rm T}(H(AP_{\rm c}A^{\rm T}+Q)\times H^{\rm T}+R_{s_i})^{-1}H)(AP_{\rm c}A^{\rm T}+Q)A^{\rm T}+Q. \tag{48}$$

For the cross-covariance P_{12}, according to (8) we have

$$P_{12} = W_1^{\rm e}P_{\rm c}(W_2^{\rm e})^{\rm T} + \sum_{i=1}^{d} W_1^{\rm v}(i)Q(W_2^{\rm v}(i))^{\rm T}. \tag{49}$$

Now $P_{\rm c}$ could be obtained by solving the simultaneous equations (35)–(36) (40)–(41)(47)(49). After that $\bar{P}_i$, K_i, P_i, P_{12}, K_{12} and $\varOmega$ could be obtained with (36)(38)(40)–(41)(48)–(49) respectively.

4.2 Multi-track case

For the multi-track case, by substituting (17) into (26) it gives that

$$\varOmega = K_N P_N K_N^{\rm T}, \tag{50}$$

where

$$K_N = (I_N^{\rm T}P_N^{-1}I_N)^{-1}(I_N^{\rm T}P_N^{-1}). \tag{51}$$

Recall that P_N is given in (4), it can be seen that each element of P_N, including P_{s_i} and $P_{s_is_j}$, can be obtained by using the similar method that we used for the two-track case. Note that it requires to replace (35) with (3) for the multi-track case.

5 Simulations and discussions

To evaluate the performance of the proposed fusion algorithms, we consider a tracking scenario with one target, four UAVs and a remote fusion center. A 1D constant velocity model for the target is given as

$$\dot{x}(t) = Fx(t) + Lq(t), \tag{52}$$

where $x=(x,\dot{x})$ and $q(t)$ is a white noise process with a power spectral density $q_{\rm c}$. In order to implement the Kalman filter[8] on each local UAV, the target model is discretized as in [16] and the measurement model is given as (28).

5.1 MSE and NEES test

The following set of parameters are used for the simulation. For the target, let $\Delta t = 1\,{\rm s}$ and $q_{\rm c} = 1\,{\rm m}^2/{\rm s}^4$. For the sensors, it is assumed that they are available to obtain the position measurements of the target with a sampling interval of 1 s and the variances of the measurement noise are $R_1=R_2=R_3=R_4=R=1\,{\rm m}^2$. Furthermore, the communication interval between the UAVs and the FC is set to be 5 s. For the FC, it would send the fused track back to the UAVs according to a specific information feedback configuration. In detail, for the configuration of no feedback, no UAV receives the feedback; for the configuration of partial feedback, only UAVs 1 and 2 receive the feedback; and for the configuration of full feedback, all the four UAVs receive the feedback.

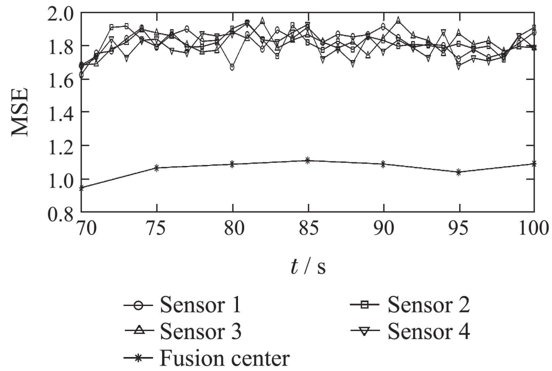

Fig. 1 MSE for the configuration of no feedback

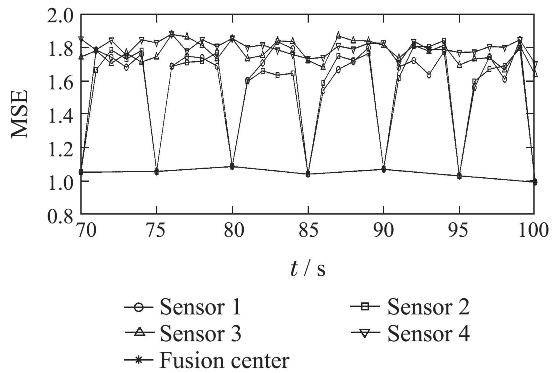

Fig. 2 MSE for the configuration of partial feedback

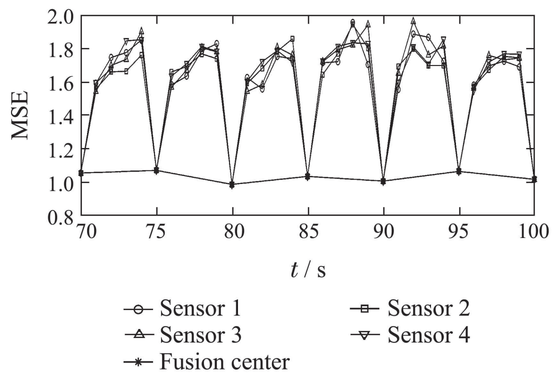

Fig. 3 MSE for the configuration of full feedback

A $1,000$ runs Monte Carlo simulation is performed to verify the effectiveness of the proposed fusion algorithm. We use the mean squared error (MSE)[8]

$$\mathrm{MSE}(k) = \frac{1}{1000}\sum_{i=1}^{1000}(\tilde{x}_{\rm c}^i(k|k))^{\rm T}\tilde{x}_{\rm c}^i(k|k) \tag{53}$$

as the performance metric. From Figs.1–3 it can be seen that the MSE for the fused track is significantly lower than the local tracks for all the three different information feedback configurations, which illustrates that the fusion algorithms improve the estimation accuracy effectively at each fusion step. With respect to the estimation consistency, Figs.4–6 show that the algorithms are consistent since most of the values are found inside the 95% confidence interval with the NEES test[16], which proves that the calculation of the cross-covariances is appropriate.

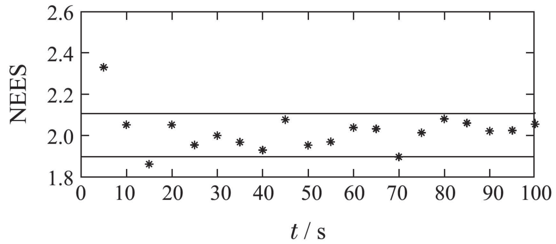

Fig. 4 NEES test for the configuration of no feedback

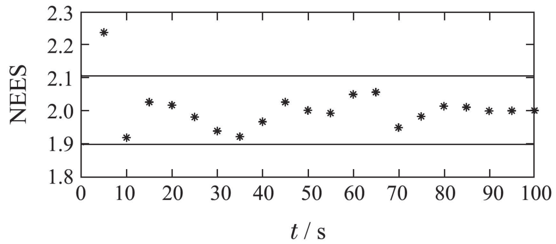

Fig. 5 NEES test for the configuration of partial feedback

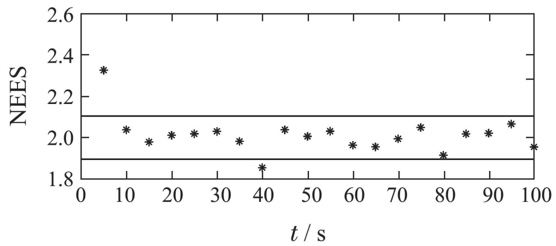

Fig. 6 NEES test for the configuration of full feedback

5.2 Steady-state performance analysis

The objective of this part is to evaluate the performance of the fusion algorithms with varying parameters. For the sake of simplicity, we mainly focus on the configurations of no feedback and full feedback. In the following, we define the averaged MSE as the mean of $\{\mathrm{MSE}(k)\}_{k=1}^{nstep}$ and the difference in rate between a and b as

$$\Delta(a,b) = \frac{|\mathrm{trace}(a) - \mathrm{trace}(b)|}{\mathrm{trace}(a)} \times 100. \quad (54)$$

Tables 1 and 2 compare the trace of the predicted steady-state MSE covariance Ω, the simulated steady-state filter covariance P_{c} and the simulated averaged MSE with varying values of q_{c}, in which q_{c} is the spectral density of process noise, and $R_1 = R_2 = R_3 = R_4 = 10$. For the configuration of no feedback, it is clear that Ω is in perfect agreement with P_{c}. Besides, there is some minor difference between the simulated averaged MSE and Ω. For the configuration of full feedback, P_{c} becomes slightly different from Ω. The difference could be due to the numerical round off error caused by inverting P_N, which is a high order matrix. There is no such calculation for the no feedback case. Besides, the difference between the simulated averaged MSE and Ω is still relatively small. Note that there is no obvious correlation between q_{c} and $\Delta(\mathrm{MSE}, \Omega)$. By comparing the result between the no feedback and full feedback case, it can be seen that the impact of information feedback is negative, namely the feedback can lead to a certain amount of loss in fusion accuracy.

Table 1 Comparison between Ω, P_{c} and the simulated averaged MSE with varying values of q_{c} for the configuration of no feedback

$q_{\mathrm{c}}/(\mathrm{m}^2\cdot\mathrm{s}^{-4})$	trace(Ω)	trace(P_{c})	trace(MSE)
1	3.6671	3.6671	3.6551
20	15.3793	15.3793	15.4045
40	23.4075	23.4075	23.3469
60	30.4756	30.4756	30.4410
80	37.0929	37.0929	37.1751
100	43.4514	43.4514	43.4074

Table 2 Comparison between Ω, P_{c} and the simulated averaged MSE with varying value of q_{c} for the configuration of full feedback

$q_{\mathrm{c}}(\mathrm{m}^2\cdot\mathrm{s}^{-4})$	trace(Ω)	trace(P_{c})	trace(MSE)
1	3.7029	3.7127	3.6982
20	15.3781	15.3804	15.3440
40	23.4077	23.4099	23.4858
60	30.4760	30.4775	30.4262
80	37.0932	37.0939	37.2282
100	43.4515	43.4517	43.3295

Tables 3 and 4 compare the trace of Ω, P_{c} and the simulated averaged MSE with different number of UAVs, in which $R_1 = R_2 = R_3 = R_4 = 1$. For the configuration of no feedback, it can be seen that Ω and P_{c} are still in perfect agreement. There is some minor difference between the simulated avraged MSE and Ω. For the configuration of full feedback, again, the difference exists between P_{c} and Ω. Furthermore, it is obvious that $\Delta(P_{\mathrm{c}}, \Omega)$ increases as the number of UAVs increases. The reason is that the order of P_N is proportional to the number of UAVs, and by inverting a higher order matrix it could induce a larger error. Besides, the difference between the simulated averaged MSE and Ω is still small. In both cases, it is obvious that the fusion accuracy can be improved by incorporating more UAVs to fuse their local tracks.

Table 3 Comparison between Ω, P_{c} and the simulated averaged MSE with different number of UAVs for the configuration of no feedback

N	trace(Ω)	trace(P_{c})	trace(MSE)
2	1.2943	1.2943	1.2878
4	1.0459	1.0459	1.0479
6	0.9631	0.9631	0.9606
8	0.9218	0.9218	0.9217
10	0.8969	0.8969	0.8975

Table 4 Comparison between Ω, P_{c} and the simulated averaged MSE with different number of UAVs for the configuration of full feedback

N	trace(Ω)	trace(P_{c})	trace(MSE)
2	1.2944	1.2947	1.2977
4	1.0462	1.0470	1.0459
6	0.9635	0.9646	0.9672
8	0.9222	0.9233	0.9209
10	0.8974	0.8986	0.9039

5.3 Comparison against existing fusion methods

In this section, the performance of the proposed multi-UAV T2TF algorithm is compared against two well-known fusion algorithms, namely the centralized Kalman filter (CKF) and the Naive fusion. While the CKF offers the optimal fusion result in the minimum mean squared error (MMSE) sense, it requires all the local measurements to be available in FC. The Naive fusion[17] is the simplest fusion method in which the correlation between the local estimations is omitted. Table 5 shows that the accuracy of the proposed fusion algorithm is higher than the Naive fusion, however it still cannot achieve the performance of CKF. In addition, although the Naive fusion performs closely to the proposed fusion algorithm in the sense of accuracy, its fused covariance is much smaller than the true one, thus it is not a consisten estimator.

Table 5 Comparison between centralized Kalman filter, Naive fusion and the proposed multi-UAV T2TF for the configuration of partial feedback ($R_1 = R_2 = R_3 = R_4 = 1$)

Fusion algorithm	Averaged MSE	Consistency
Centralized Kalman filter	0.8941	Yes
Naive fusion	1.2486	No
Multi-UAV T2TF	1.2209	Yes

5.4 Discussion of the application of the multi-UAV T2TF algorithms

While the effectiveness of the proposed multi-UAV T2TF algorithms have been evaluated in the above simulations, it's essential to discuss several potential isssues for its realization to the practical environment. Firstly, the way this system solves the T2TF problem requires frequent use of communication bandwidth between the local UAVs and the FC, which is less practical due to the bandwidth and power limitations in reality, hence it is promising to introduce the event-based estimation techniques to reduce the communication load. Secondly, local UAVs might communicate with FC at different rates, which raises the problem of asynchronous T2TF. In the end, the treatment of correlation between local estimates becomes more complicated for the nonlinear estimation problem, while linear fusion only requires the calculation of the cross-covariances matrix, the exact correlation between the nonlinear estimates has to be represented by high-dimensional probability density functions (PDFs), which is more difficult to store and keep track of. So it is challenging to find a strategy for suboptimal representation of the correlation between the local nonlinear estimates.

6 Conclusions

In this paper, formulas are derived to calculate the exact cross-covariances between local tracks for various information configurations in a multiple UAVs network. Based on the derived formulas, the consistent track-to-track fusion algorithms are developed which can operate at arbitrary communication rate. The steady-state fusion performance of the developed algorithms for specific information feedback configurations is predicted by solving the corresponding discrete algebraic Riccati equations. Extensive Monte Carlo simulation is conducted to verify the proposed algorithms.

References:

[1] WHEELER M, SCHRICK B, WHITACRE W, et al. Cooperative tracking of moving targets by a team of autonomous uavs [C] //*The 25th Digital Avionics Systems Conference*, Portland: IEEE/AIAA, 2006: 1 – 9.

[2] CHEN H, KIRUBARAJAN T, BAR-SHALOM Y. Performance limits of track-to-track fusion versus centralized estimation: theory and application [J]. *IEEE Transactions on Aerospace and Electronic Systems*, 2003, 39(2): 386 – 400.

[3] GAO Y, KRAKIWSKY E, ABOUSALEM M, et al. Comparison and analysis of centralized, decentralized, and federated filters [J]. *Navigation*, 1993, 40(1): 69 – 86.

[4] KIM K H. Development of track to track fusion algorithms [C] //*American Control Conference*. Baltimore: IEEE, 1994: 1037 – 1041.

[5] GOVAERS F, KOCH W. An exact solution to track-to-track-fusion at arbitrary communication rates [J]. *IEEE Transactions on Aerospace and Electronic Systems*, 2012, 48(3): 2718 – 2729.

[6] BAR-SHALOM Y. On the track-to-track correlation problem [J]. *IEEE Transactions on Automatic Control*, 1981, 26(2): 571 – 572.

[7] BAR-SHALOM Y, CAMPO L. The effect of the common process noise on the two-sensor fused-track covariance [J]. *IEEE Transactions on Aerospace and Electronic Systems*, 1986, 22(6): 803 – 805.

[8] BAR-SHALOM Y, LI X R. *Estimation and Tracking — Principles, Techniques, and Software* [M]. Norwood, MA: Artech House, Inc, 1993.

[9] CHANG K C, SAHA R K, BAR-SHALOM Y. On optimal track-to-track fusion [J]. *IEEE Transactions on Aerospace and Electronic Systems*, 1997, 33(4): 1271 – 1276.

[10] CHANG K C. Evaluating hierarchical track fusion with information matrix filter [C] //*Proceedings of the 3rd International Conference on Information Fusion*. Paris: IEEE, 2000: MOC2/3 – MOC2.9.

[11] DENG Z, ZHANG P, QI W, et al. The accuracy comparison of multisensor covariance intersection fuser and three weighting fusers [J]. *Information Fusion*, 2013, 14(2): 177 – 185.

[12] CHANG K C, ZHI T, SAHA R K. Performance evaluation of track fusion with information matrix filter [J]. *IEEE Transactions on Aerospace and Electronic Systems*, 2002, 38(2): 455 – 466.

[13] NIEHSEN W. Information fusion based on fast covariance intersection filtering [C] //*Proceedings of the 5th International Conference on Information Fusion*. Annapolis: IEEE, 2002: 901 – 904.

[14] TIAN X, BAR-SHALOM Y. Exact algorithms for four track-to-track fusion configurations: All you wanted to know but were afraid to ask [C] //*The 12th International Conference on Information Fusion*. Seattle: IEEE, 2009: 537 – 544.

[15] TIAN X, BAR-SHALOM Y. On algorithms for asynchronous track-to-track fusion [C] // *The 13th International Conference on Information Fusion*. Edinburgh: IEEE, 2010: 1 – 8.

[16] BAR-SHALOM Y, LI X R, KIRUBARAJAN T. *Estimation with Applications to Tracking and Navigation: Theory Algorithms and Software* [M]. Hoboken: John Wiley & Sons, 2004.

[17] CHANG K C, CHONG C Y, MORI S. On scalable distributed sensor fusion [C] // *The 11th International Conference on Information Fusion*. Cologne: IEEE, 2008: 1 – 8

作者简介:

陆科林 (1987–), 男, 博士研究生, 目前研究方向为航迹融合, E-mail: klu@buaa.edu.cn;

周 锐 (1968–), 男, 教授, 目前研究方向为无人机自主控制、多飞行器协同控制等, E-mail: zhr@buaa.edu.cn;

张翔伦 (1971–), 女, 研究员, 目前研究方向为飞行控制系统控制律设计、无人机自主控制等, E-mail: zh_xl_2007@hotmail.com.